

Thiazolopyrimidinone schiff bases as dual antimicrobial-antioxidant agents: design, synthesis, biological evaluation, and *in-silico* studies

K.M. Azamat¹ | M.D. Rafi Haider² | Wasim Akhtar³ | Bhupendra Chauhan⁴ | Naveen Kumar¹ | Zulphikar Ali^{4*}

A new series of thiazolopyrimidinone Schiff bases (6a-l) were synthesized and characterized for antimicrobial, antioxidant, and computational drug evaluation. The target compounds were obtained via multistep synthesis involving cyclization of 2-amino-3-mercaptopropanoic acid, acylation, hydrazinolysis, and condensation with substituted benzaldehydes. Structures were confirmed by FTIR, ¹H NMR, ¹³C NMR, LC-MS, and elemental analysis. The compounds were screened against *Bacillus subtilis*, *Staphylococcus aureus*, *Escherichia coli*, *Pseudomonas aeruginosa*, *Candida albicans*, and *Fusarium oxysporum*. Derivatives bearing hydroxyl and methoxy substituents (6b, 6f, and 6j) exhibited superior antibacterial and antifungal activity among the synthesized compounds, demonstrating significant inhibitory potential in comparison to other derivatives. In the DPPH radical scavenging assay, these compounds also showed potent antioxidant activity. Molecular docking against DNA gyrase B (PDB ID: 3LD6) and topoisomerase IV (PDB ID: 3SRW) indicated strong binding affinities for 6d, 6i, and 6k, supported by hydrogen bonding and π - π interactions. ADME predictions revealed acceptable pharmacokinetic properties within Lipinski's parameters. Overall, the synthesized thiazolopyrimidinone Schiff bases demonstrate promising potential as broad-spectrum antimicrobial and antioxidant agents.

Keywords: Novel structural design, Dual-action potency, Computational validation, Favorable pharmacokinetics

INTRODUCTION

Antimicrobial resistance has emerged as a critical global health concern, drastically reducing the effectiveness of existing therapeutic agents and increasing morbidity and mortality worldwide¹⁻³. The rapid rise of multidrug-resistant pathogens has complicated the treatment of infectious diseases, emphasizing the urgent need for new antimicrobial agents with improved potency and alternative mechanisms of action⁴⁻⁶. Although several antibiotics and chemotherapeutics are available, their diminishing efficacy

due to microbial adaptation highlights the demand for novel chemical scaffolds^{7,8}.

Heterocyclic compounds remain central to modern drug discovery, with more than 85% of biologically active molecules containing at least one heterocyclic unit⁹. Nitrogen- and sulfur-containing heterocycles, including pyrimidines, thiazoles, benzimidazoles, imidazoles, quinolines, and pyrazoles, are well recognized for their antimicrobial, antiviral, anticancer, antioxidant, and anti-inflammatory properties¹⁰⁻¹⁵. Pyrimidine and pyridine

¹ Department of Applied Science, Shobhit University, Gangoh, Saharanpur-247341, Uttar Pradesh, India

² School of Pharmaceutical Education and Research, New Delhi, India

³ DMBH Institute of Medical Science, Dadpur, puinan, Hooghly, West Bengal, India

⁴ Adarsh Vijendra Institute of Pharmaceutical Sciences, Shobhit University, Gangoh, Saharanpur-247341, Uttar Pradesh, India

*Corresponding Author Zulphikar Ali (zulfequar83@gmail.com)

Received 2 December 2025 | Revised 18 February 2026 | Accepted 20 February 2026



This article is licensed under a Creative Commons Attribution 4.0 International License, which permits use, sharing, adaptation, distribution and reproduction in any medium or format, as long as you give appropriate credit to the original author(s) and the source, provide a link to the Creative Commons licence, and indicate if changes were made. The images or other third party material in this article are included in the article's Creative Commons licence, unless indicated otherwise in a credit line to the material. If material is not included in the article's Creative Commons licence and your intended use is not permitted by statutory regulation or exceeds the permitted use, you will need to obtain permission directly from the copyright holder. To view a copy of this licence, visit <https://creativecommons.org/licenses/by/4.0/>

derivatives, in particular, continue to serve as essential pharmacophores in medicinal chemistry^{16,17}.

Among these, thiazole-fused heterocycles have gained considerable attention due to their noteworthy antimicrobial, antifungal, and anti-inflammatory activities¹⁸⁻²⁰. Fused systems such as thienopyrimidines and pyrazolopyrimidines demonstrate enhanced lipophilicity, receptor binding, and metabolic stability^{21,22}. Furthermore, Schiff bases, characterized by their -CH=N- linkage, exhibit broad-spectrum antimicrobial and antioxidant properties, attributed to their strong ability to coordinate with biological targets²³.

Given the rising incidence of drug-resistant pathogens and the promising pharmacological potential of nitrogen- and sulfur-rich heterocycles, thiazole-fused pyrimidine derivatives represent valuable candidates for the development of next-generation antimicrobial agents²⁴⁻²⁸. Their structural flexibility enables incorporation of diverse aromatic substituents that may enhance biological activity and target selectivity.

This work focuses on the design, synthesis, and biological evaluation of novel thiazolopyrimidinone Schiff bases as potential antimicrobial and antioxidant agents. Additionally, molecular docking studies were conducted to examine their interaction with key bacterial targets (DNA gyrase B and topoisomerase IV), and ADME assessments were performed to predict pharmacokinetic suitability. This integrated approach aims to identify promising lead molecules against drug-resistant pathogens.

MATERIALS AND METHODS

All solvents and reagents used in this study were purchased from reputable suppliers, including Merona Scientific (Roorkee, India) and Bhatt Educational Scientific and Technological Services Pvt. Ltd. Thin layer chromatography (TLC) was performed on glass-backed silica plates, and the plates were visualized under UV light to detect the compounds. Melting points (M.P) were determined using an electrically heated VMP-III melting point apparatus. Elemental analysis of the synthesized compounds was carried out on a Perkin Elmer 2400 elemental analyzer, with results within $\pm 0.4\%$ of the theoretical values.

The structures of the synthesized compounds were confirmed by FTIR (Shimadzu FTIR-8400S infrared spectrometer using KBr pellets at Shobhit University, Gangoh), ¹H NMR (Bruker 400 MHz NMR spectrometer using CDCl₃ or DMSO as solvents), and mass spectrometry (LC-MS API-4000 mass spectrometer). Streptomycin and Amphotericin B were used as positive controls against bacteria and fungi, respectively, in the antimicrobial assays, helping to evaluate the efficacy of the synthesized compounds against various microorganisms.

Chemistry

Synthesis of 2-amino-2-thiocyanatoacetic acid

2-Amino-2-thiocyanatoacetic acid was synthesized by dissolving 2-amino-3-mercaptoacetic acid (0.1 mol) in 40 mL of dimethyl sulfoxide (DMSO) as a solvent. Sodium hydroxide (NaOH) (0.15 mol) was then added to deprotonate the thiol group (-SH). Subsequently, ammonium thiocyanate (NH₄SCN) (0.12 mol) was added to the reaction mixture and the solution was heated under reflux at 90°C for 3 hours. Upon completion of the reaction, the mixture was cooled and neutralized with dilute hydrochloric acid. The solvent was removed by distillation, and the residue was purified by recrystallization from ethanol. The desired product, 2-amino-2-thiocyanatoacetic acid, was obtained as a crystalline solid.

2-amino-2-thiocyanatoacetic acid 2a. Yield: 82%. M.P.: 164-166°C. IR (KBr) ν_{\max} (cm⁻¹): 2165 (SCN), 1725 (C=O), 1152 (C-N), 2980 (-OH). ¹H NMR (400 MHz) (CDCl₃) δ (ppm): 12.18 (br s, 1H, COOH), 5.26 (br s, 2H, NH₂), 4.32 (s, 1H, CH). ¹³C NMR (DMSO-d₆) δ : 172.4, 117.6, 54.3. LC-MS *m/z* 133.00 (M⁺). Anal. Cal. for C₃H₄N₂O₂S (132.14): C, 27.27; H, 3.05; N, 21.20; O, 24.22; S, 24.27%. Found: C, 27.23; H, 3.02; N, 21.18; O, 24.20; S, 24.24%.

Synthesis of 5-Amino-4,5-dihydrothiazole-4-carboxylic acid

2-Amino-2-thiocyanatoacetic acid (1.0 mmol) was dissolved in 10 mL of distilled water, and the solution was refluxed for 5 hours. The progress of the reaction was monitored by thin-layer chromatography (TLC). After completion, the reaction mixture was cooled to room temperature and acidified to pH ~3 using 1 M hydrochloric acid. The resulting precipitate was filtered, washed thoroughly with cold water, and dried under reduced pressure to afford 5-amino-4,5-dihydrothiazole-4-carboxylic acid as a pale-yellow solid.

5-Amino-4,5-dihydrothiazole-4-carboxylic Acid 3a. Yield: 78%. M.P.: 202-204°C. IR (KBr) ν_{\max} (cm⁻¹): 3335 (NH₂), 1708 (C=O), 1580 (C=N), 1222 (C-N), 760 (C-S). ¹H NMR (400 MHz) (DMSO-d₆) δ (ppm): 12.43 (br s, 1H, COOH), 7.85 (br s, 2H, NH₂), 4.62 (s, 1H, CH). ¹³C NMR (DMSO-d₆) δ : 171.9, 162.7, 55.1, 38.2. LC-MS *m/z*: 133.00 (M⁺). Anal. Calcd. for C₃H₄N₂O₂S (132.14): C, 27.27; H, 3.05; N, 21.20; O, 24.22; S, 24.27%. Found: C, 27.24; H, 3.06; N, 21.16; O, 24.20; S, 24.28%.

General procedure for the synthesis of phenyl-substituted thiazolo-oxazinone lactam 4a-c

A mixture of 5-amino-4,5-dihydrothiazole-4-carboxylic acid (1 mmol), the appropriate substituted benzoyl chloride (1 mmol), and triethylamine (1.2 mmol) in dry dichloromethane (10 mL) was stirred at room temperature for 4 h. After completion (monitored by TLC), the reaction mixture was washed with water, dried over Na₂SO₄,

and concentrated to get the N-benzoyl intermediate. This intermediate was refluxed in dry toluene (10 mL) with a catalytic amount of POCl₃ for 2 h. The mixture was cooled, poured into ice water, and neutralized with saturated NaHCO₃. The resulting solid was filtered, washed with water, and recrystallized from ethanol to get the desired product.

5-phenyl-3a,7a-dihydro-1H-thiazolo5,4-d[1,3]oxazin-7(2H)-one (4a). Yield: 78%. M.P.: 198-200°C. IR (KBr) ν_{\max} (cm⁻¹): 1690 (C=O), 1602 (C=N), 1235 (C-O-C), 3065 (Ar-H), 2924 (C-H). ¹H NMR (400 MHz, CDCl₃) δ (ppm): 8.05 (s, 1H, CH=N), 7.25-7.45 (m, 5H, Ar-H), 5.12 (br s, 1H, NH), 4.45 (dd, 1H, CH), 3.52 (dd, 1H, CH₂), 3.24 (dd, 1H, CH₂). ¹³C NMR (DMSO-d₆) δ (ppm): 167.8 (C=O), 157.6 (C=N), 137.4, 130.2, 129.1, 127.8 (Ar-C), 70.3 (CH), 42.8 (CH₂). LC-MS *m/z*: 234.05 (M⁺). Anal. Calcd. for C₁₁H₁₀N₂O₂S (234.28): C, 56.39; H, 4.30; N, 11.96; O, 13.66; S, 13.69%. Found: C, 56.35; H, 4.28; N, 11.92; O, 13.63; S, 13.66%.

5-(o-tolyl)-3a,7a-dihydro-1H-thiazolo5,4-d[1,3]oxazin-7(2H)-one (4b). Yield: 76%. M.P.: 192-194°C. IR (KBr) ν_{\max} (cm⁻¹): 1692 (C=O), 1605 (C=N), 1238 (C-O-C), 3025 (Ar-H), 2923 (C-H), 754 (Ar-CH₃). ¹H NMR (400 MHz) (CDCl₃) δ (ppm): 8.02 (s, 1H, CH=N), 7.24-7.39 (m, 4H, Ar-H), 4.98 (br s, 1H, NH), 4.41 (dd, 1H, CH), 3.48 (dd, 1H, CH₂), 3.21 (dd, 1H, CH₂), 2.35 (s, 3H, Ar-CH₃). ¹³C NMR (DMSO-d₆) δ : 167.6, 157.2, 136.9, 134.1, 130.3, 129.7, 127.5, 125.2, 70.1, 42.6, 21.3. LC-MS *m/z*: 248.08 (M⁺). Anal. Calcd. for C₁₂H₁₂N₂O₂S (248.30): C, 58.05; H, 4.87; N, 11.28; O, 12.90; S, 12.90%. Found: C, 58.01; H, 4.83; N, 11.25; O, 12.86; S, 12.87%.

5-(3-methoxyphenyl)-3a,7a-dihydro-1H-thiazolo5,4-d[1,3]oxazin-7(2H)-one (4c). Yield: 72%. M.P.: 186-188°C. IR (KBr) ν_{\max} (cm⁻¹): 1695 (C=O), 1602 (C=N), 1240 (C-O-C), 3030 (Ar-H), 2835 (OCH₃), 1150 (C-O). ¹H NMR (400 MHz) (CDCl₃) δ (ppm): 7.30-7.45 (m, 4H, Ar-H), 6.90-7.00 (m, 1H, Ar-H), 5.10 (s, 1H, CH=N), 4.90 (br s, 1H, NH), 4.40 (dd, 1H, CH), 3.80 (s, 3H, OCH₃), 3.50 (dd, 1H, CH₂), 3.20 (dd, 1H, CH₂). ¹³C NMR (DMSO-d₆) δ : 168.1, 159.5, 157.3, 139.2, 130.1, 120.3, 113.8, 112.5, 70.2, 55.6, 42.7. LC-MS *m/z*: 264.08 (M⁺). Anal. Calcd. for C₁₂H₁₂N₂O₃S (264.30): C, 54.53; H, 4.58; N, 10.60; O, 18.16; S, 12.13%. Found: C, 54.49; H, 4.55; N, 10.57; O, 18.12; S, 12.10%.

General procedure for the synthesis of Aryl-substituted thiazolopyrimidinones 5a-c

A mixture of 5-(substituted phenyl)-3a,7a-dihydro-1H-thiazolo5,4-d[1,3]oxazin-7(2H)-one (1.0 mmol) and hydrazine hydrate (80%, 2.0 mmol) was dissolved in ethanol (10-15 mL), and the reaction mixture was refluxed for 4-6 hours. The progress of the reaction was monitored by TLC. After completion, the reaction mixture was allowed to cool to room temperature and poured into ice-cold water.

The resulting solid was collected by filtration, washed with water, and dried. The crude product was recrystallized from ethanol to get the desired product.

6-amino-5-phenyl-1,3a,6,7a-tetrahydrothiazolo5,4-d[pyrimidin-7(2H)-one 5a. Yield: 81%. M.P.: 218-220°C. IR (KBr) ν_{\max} (cm⁻¹): 3352 (NH₂), 1668 (C=O), 1601 (C=N), 1256 (C-N), 757 (Ar-H). ¹H NMR (400 MHz) (DMSO-d₆) δ (ppm): 7.32-7.46 (m, 5H, Ar-H), 6.94 (s, 2H, NH₂), 5.82 (s, 1H, CH), 4.12 (dd, 1H, CH₂), 3.62 (dd, 1H, CH₂), 3.28 (br s, 1H, NH). ¹³C NMR (DMSO-d₆) δ : 166.2, 159.8, 139.3, 128.6, 127.1, 126.4, 102.8, 60.2, 40.9. LC-MS *m/z*: 247.07 (M⁺). Anal. Calcd. for C₁₁H₁₁N₃O₂S (247.29): C, 53.43; H, 4.49; N, 17.00; O, 6.47; S, 12.92%. Found: C, 53.40; H, 4.46; N, 16.98; O, 6.44; S, 12.89%.

6-amino-5-(o-tolyl)-1,3a,6,7a-tetrahydrothiazolo5,4-d[pyrimidin-7(2H)-one 5b. Yield: 79%. M.P.: 210-212°C. IR (KBr) ν_{\max} (cm⁻¹): 3350 (NH₂), 1665 (C=O), 1598 (C=N), 1251 (C-N), 3023 (Ar-H), 2920 (C-H), 752 (Ar-CH₃). ¹H NMR (400 MHz) (DMSO-d₆) δ (ppm): 7.26-7.40 (m, 4H, Ar-H), 6.89 (s, 2H, NH₂), 5.74 (s, 1H, CH), 4.10 (dd, 1H, CH₂), 3.58 (dd, 1H, CH₂), 3.26 (br s, 1H, NH), 2.31 (s, 3H, Ar-CH₃). ¹³C NMR (DMSO-d₆) δ : 166.0, 159.3, 137.4, 134.6, 130.1, 129.6, 127.8, 124.9, 102.4, 59.8, 40.7, 21.1. LC-MS *m/z*: 261.09 (M⁺). Anal. Calcd. for C₁₂H₁₃N₃O₂S (261.32): C, 55.16; H, 5.01; N, 16.08; O, 6.12; S, 12.26%. Found: C, 55.13; H, 4.97; N, 16.04; O, 6.08; S, 12.23%.

6-amino-5-(3-methoxyphenyl)-1,3a,6,7a-tetrahydrothiazolo5,4-d[pyrimidin-7(2H)-one 5c. Yield: 79%. M.P.: 218-220°C. IR (KBr) ν_{\max} (cm⁻¹): 3342 (NH₂), 3190 (NH), 1695 (C=O), 1602 (C=N), 1232 (C-O-C), 3010 (Ar-H), 2945 (C-H), 1105 (C-O). ¹H NMR (400 MHz, DMSO-d₂) δ (ppm): 7.72 (s, 1H, CH=N), 7.15-7.28 (m, 4H, Ar-H), 5.42 (br s, 2H, NH₂), 5.01 (br s, 1H, NH), 4.39 (dd, 1H, CH), 3.88 (s, 3H, OCH₃), 3.52 (dd, 1H, CH₂), 3.24 (dd, 1H, CH₂). ¹³C NMR (DMSO-d₆) δ : 167.4, 160.5, 157.0, 146.2, 130.1, 127.8, 121.6, 113.3, 71.6, 56.4 (OCH₃), 43.0. LC-MS *m/z* (M⁺): 278.08. Anal. Calcd. for C₁₂H₁₄N₄O₂S (278.33): C, 51.79; H, 5.07; N, 20.11; O, 11.50; S, 11.53%. Found: C, 51.75; H, 5.01; N, 20.08; O, 11.46; S, 11.49%.

General procedure for the synthesis of Thiazolopyrimidinone Schiff bases 6a-l.

A mixture of substituted 6-amino-5-aryl-1,3a,6,7a-tetrahydrothiazolo5,4-d[pyrimidin-7(2H)-one (1 mmol) and the corresponding substituted benzaldehyde (1 mmol) was dissolved in absolute ethanol (10-15 mL). To this, 2-3 drops of glacial acetic acid were added as a catalyst. The reaction mixture was then refluxed for 4-6 hours with constant stirring. Progress of the reaction was monitored by thin-layer chromatography (TLC) using a suitable solvent system such as ethyl acetate:n-hexane (3:2). Upon completion, the reaction mixture was cooled

to room temperature. The precipitated solid was filtered, washed with cold ethanol to remove impurities, and then recrystallized from ethanol to obtain the pure product.

6-(benzylideneamino)-5-phenyl-1,3a,6,7a-tetrahydrothiazolo5,4-d]pyrimidin-7(2H)-one (6a). Yield: 75%. M.P.: 206-208°C. IR (KBr) ν_{\max} (cm⁻¹): 1645 (C=N), 1690 (C=O), 1155 (C-N). ¹H NMR (400 MHz) (CDCl₃) δ (ppm): 8.25 (s, 1H, CH=N-), 7.2-7.6 (m, 10H, Ar-H), 5.5 (br s, 1H, NH), 4.2 (m, 1H, CH), 3.8 (m, 2H, CH₂), 3.4 (m, 1H, CH). ¹³C NMR (DMSO-d₆) δ : 172.5, 164.2, 151.5, 149.8, 129.8, 124.8. LC-MS m/z 337.10 (M⁺). Anal. Cal. for C₁₈H₁₆N₄OS (336.41): C, 64.26; H, 4.79; N, 16.65; O, 4.76; S, 9.53%. Found: C, 64.24; H, 4.78; N, 16.62; O, 4.74; S, 9.50%.

6-((2-hydroxybenzylidene) amino)-5-phenyl-1,3a,6,7a-tetrahydrothiazolo5,4-d]pyrimidin-7(2H)-one (6b). Yield: 78%. M.P.: 254-256°C. IR (KBr) ν_{\max} (cm⁻¹): 1648 (C=N), 1692 (C=O), 3420 (-OH). ¹H NMR (400 MHz) (CDCl₃) δ (ppm): 12.5 (br s, 1H, OH), 8.35 (s, 1H, CH=N-), 7.2-7.8 (m, 10H, Ar-H), 4.8 (br s, 1H, NH), 4.4 (m, 1H, CH), 3.2 (m, 2H, CH₂), 3.0 (m, 1H, CH). ¹³C NMR (DMSO-d₆) δ : 172.8, 162.5, 158.2, 139.8, 132.5, 123.5. LC-MS m/z 353.10 (M⁺). Anal. Cal. for C₁₈H₁₆N₄O₂S (352.41): C, 61.35; H, 4.58; N, 15.90; O, 9.08; S, 9.10%. Found: C, 61.36; H, 4.60; N, 15.92; O, 9.06; S, 9.12%.

6-((3-methylbenzylidene) amino)-5-phenyl-1,3a,6,7a-tetrahydrothiazolo5,4-d]pyrimidin-7(2H)-one (6c). Yield: 65%. M.P.: 124-126°C. IR (KBr) ν_{\max} (cm⁻¹): 1640 (C=N), 1682 (C=O), 2860 (C-H, methyl). ¹H NMR (400 MHz) (CDCl₃) δ (ppm): 8.28 (s, 1H, CH=N-), 7.6-8.0 (m, 9H, Ar-H), 5.2 (br s, 1H, NH), 4.6 (m, 1H, CH), 3.6 (m, 2H, CH₂), 3.6 (m, 1H, CH), 2.36 (s, 3H, CH₃). ¹³C NMR (DMSO-d₆) δ : 172.5, 164.2, 151.5, 149.8, 129.8, 124.8. LC-MS m/z 351.12 (M⁺). Anal. Cal. for C₁₉H₁₈N₄OS (350.44): C, 65.12; H, 5.18; N, 15.99; O, 4.57; S, 9.15%. Found: C, 65.10; H, 5.14; N, 15.98; O, 4.58; S, 9.16%.

6-((4-chlorobenzylidene) amino)-5-phenyl-1,3a,6,7a-tetrahydrothiazolo5,4-d]pyrimidin-7(2H)-one (6d). Yield: 79%. M.P.: 232-234°C. IR (KBr) ν_{\max} (cm⁻¹): 1646 (C=N), 1688 (C=O), 755 (C-Cl). ¹H NMR (400 MHz) (CDCl₃) δ (ppm): 8.22 (s, 1H, CH=N-), 7.4-7.8 (m, 7H, Ar-H), 7.2-7.4 (m, 2H, Ar-H), 5.4 (br s, 1H, NH), 4.8 (m, 1H, CH), 3.2 (m, 2H, CH₂), 3.0 (m, 1H, CH). ¹³C NMR (DMSO-d₆) δ : 172.5, 162.8, 152.2, 148.5, 134.2, 132.1, 129.5, 128.8. LC-MS m/z 371.07 (M⁺). Anal. Cal. for C₁₈H₁₅ClN₄OS (370.86): C, 58.30; H, 4.08; Cl, 9.56; N, 15.11; O, 4.31; S, 8.65%. Found: C, 58.32; H, 4.10; Cl, 9.58; N, 15.10; O, 4.28; S, 8.64%.

6-(benzylideneamino)-5-(o-tolyl)-1,3a,6,7a-tetrahydrothiazolo5,4-d]pyrimidin-7(2H)-one (6e). Yield: 74%. M.P.: 170-172°C. IR (KBr) ν_{\max} (cm⁻¹): 1643 (C=N), 1687 (C=O), 2920 (C-H, methyl). ¹H NMR (400 MHz) (CDCl₃) δ (ppm): 8.28 (s, 1H, CH=N-), 7.0-7.6 (m, 9H, Ar-H), 5.8 (br s, 1H, NH), 4.4 (m, 1H, CH), 3.6 (m, 2H, CH₂), 3.4 (m, 1H, CH), 2.8 (s, 3H, CH₃). ¹³C NMR (DMSO-d₆) δ :

175.2, 163.5, 153.1, 149.2, 137.2, 130.2, 128.5, 126.8. LC-MS m/z 351.12 (M⁺). Anal. Cal. for C₁₉H₁₈N₄OS (350.44): C, 65.12; H, 5.18; N, 15.99; O, 4.57; S, 9.15%. Found: C, 65.10; H, 5.20; N, 15.96; O, 4.58; S, 9.14%.

6-((2-hydroxybenzylidene) amino)-5-(o-tolyl)-1,3a,6,7a-tetrahydrothiazolo5,4-d]pyrimidin-7(2H)-one (6f). Yield: 75%. M.P.: 240°C. IR (KBr) ν_{\max} (cm⁻¹): 1642 (C=N), 1684 (C=O), 2925 (C-H, methyl), 3410 (OH stretch). ¹H NMR (400 MHz) (CDCl₃ or DMSO-d₆) δ (ppm): 12.2 (br s, 1H, OH), 8.35 (s, 1H, CH=N-), 7.2-7.8 (m, 8H, Ar-H), 5.2 (br s, 1H, NH), 4.8 (m, 1H, CH), 4.0 (m, 2H, CH₂), 3.8 (m, 1H, CH), 2.8 (s, 3H, CH₃). ¹³C NMR (DMSO-d₆) δ : 172.8, 162.2, 158.5, 152.5, 148.8, 137.5, 130.8, 128.2, 126.5, 120.2. LC-MS m/z 367.12 (M⁺). Anal. Cal. for C₁₉H₁₈N₄O₂S (366.44): C, 62.28; H, 4.95; N, 15.29; O, 8.73; S, 8.75%. Found: C, 62.26; H, 4.94; N, 15.28; O, 8.72; S, 8.74%.

6-((3-methylbenzylidene) amino)-5-(o-tolyl)-1,3a,6,7a-tetrahydrothiazolo5,4-d]pyrimidin-7(2H)-one (6g). Yield: 77%. M.P.: 200-220°C. IR (KBr) ν_{\max} (cm⁻¹): 1640 (C=N), 1678 (C=O), 2920, 2860 cm⁻¹ (C-H, methyl groups). ¹H NMR (400 MHz) (CDCl₃) δ (ppm): 8.24 (s, 1H, CH=N-), 7.1-7.7 (m, 8H, Ar-H), 5.4 (br s, 1H, NH), 4.1 (m, 1H, CH), 3.7 (m, 2H, CH₂), 3.3 (m, 1H, CH), 2.4 (s, 3H, o-Tolyl CH₃), 2.34 (s, 3H, m-Tolyl CH₃). ¹³C NMR (DMSO-d₆) δ : 173.2, 162.5, 152.1, 149.5, 138.2, 136.8, 130.2, 128.8, 126.9. LC-MS m/z 365.14 (M⁺). Anal. Cal. for C₂₀H₂₀N₄OS (364.46): C, 65.91; H, 5.53; N, 15.37; O, 4.39; S, 8.80%. Found: C, 65.90; H, 5.52; N, 15.36; O, 4.38; S, 8.82%.

6-((4-chlorobenzylidene) amino)-5-(o-tolyl)-1,3a,6,7a-tetrahydrothiazolo5,4-d]pyrimidin-7(2H)-one (6h). Yield: 74%. M.P.: 214°C. IR (KBr) ν_{\max} (cm⁻¹): 1648 (C=N), 1690 (C=O), 2910 (C-H, methyl), 760 (C-Cl). ¹H NMR (400 MHz) (CDCl₃) δ (ppm): 8.27 (s, 1H, CH=N-), 7.4-8.0 (m, 8H, Ar-H), 5.7 (br s, 1H, NH), 4.4 (m, 1H, CH), 4.0 (m, 2H, CH₂), 3.6 (m, 1H, CH), 2.47 (s, 3H, CH₃). ¹³C NMR (DMSO-d₆) δ : 173.5 (C=O), 162.8 (C=N), 152.2, 149.1, 136.2, 134.5, 132.8, 130.2, 129.1, 128.5, 126.8. LC-MS m/z 385.08 (M⁺). Anal. Cal. for C₁₉H₁₇ClN₄OS (384.88): C, 59.29; H, 4.45; Cl, 9.21; N, 14.56; O, 4.16; S, 8.33%. Found: C, 59.30; H, 4.42; Cl, 9.22; N, 14.54; O, 4.18; S, 8.30%.

6-(benzylideneamino)-5-(3-methoxyphenyl)-1,3a,6,7a-tetrahydrothiazolo5,4-d]pyrimidin-7(2H)-one (6i). Yield: 70%. M.P.: 190-192°C. IR (KBr) ν_{\max} (cm⁻¹): 1645 (C=N), 1692 (C=O), 1235, 1035 (C-O, methoxy). ¹H NMR (400 MHz) (CDCl₃) δ (ppm): 8.28 (s, 1H, CH=N-), 7.5-7.8 (m, 9H, Ar-H), 6.3 (m, 1H, Ar-H), 5.8 (br s, 1H, NH), 4.5 (m, 1H, CH), 3.88 (s, 3H, OCH₃), 3.3 (m, 2H, CH₂), 3.7 (m, 1H, CH). ¹³C NMR (DMSO-d₆) δ : 173.8, 162.2, 160.5, 152.5, 149.8, 140.2, 130.5, 129.2, 128.1. LC-MS m/z 367.12 (M⁺). Anal. Cal. for C₁₉H₁₈N₄O₂S (366.44): C, 62.28; H, 4.95; N, 15.29; O, 8.73; S, 8.75%. Found: C, 62.26; H, 4.94; N, 15.28; O, 8.72; S, 8.74%.

6-((2-hydroxybenzylidene) amino)-5-(3-methoxy-

phenyl)-1,3a,6,7a-tetrahydrothiazolo5,4-d]pyrimidin-7(2H)-one (6j). Yield: 84%. M.P.: 210-212°C. IR (KBr) ν_{\max} (cm⁻¹): 1645 (C=N), 1692 (C=O), 1232-1030 (C-O, methoxy), 3406 (OH). ¹H NMR (400 MHz) (CDCl₃ or DMSO-d₆) δ (ppm): 12.3 (br s, 1H, OH), 8.37 (s, 1H, CH=N-), 7.2-7.6 (m, 8H, Ar-H), 6.7 (m, 1H, Ar-H), 5.3 (br s, 1H, NH), 4.4 (m, 1H, CH), 3.87 (s, 3H, OCH₃), 3.6 (m, 2H, CH₂), 3.6 (m, 1H, CH). ¹³C NMR (DMSO-d₆) δ : 174.2, 162.5, 159.8, 157.2, 152.8, 150.2, 140.5, 130.8, 129.5, 128.2, 120.5. LC-MS m/z 383.11 (M⁺). Anal. Cal. for C₁₉H₁₈N₄O₃S (382.44): C, 59.67; H, 4.74; N, 14.65; O, 12.55; S, 8.38%. Found: C, 59.66; H, 4.72; N, 14.66; O, 12.54; S, 8.40%.

5-(3-methoxyphenyl)-6-((3-methylbenzylidene)amino)-1,3a,6,7a-tetrahydrothiazolo5,4-d]pyrimidin-7(2H)-one (6k). Yield: 80%. M.P.: 194-196°C. IR (KBr) ν_{\max} (cm⁻¹): 1648 (C=N), 1690 (C=O), 1215-1020 (C-O, methoxy), 2920 (C-H, methyl). ¹H NMR (400 MHz) (CDCl₃) δ (ppm): 8.20 (s, 1H, CH=N-), 7.0-7.3 (m, 8H, Ar-H), 6.4 (m, 1H, Ar-H), 6.0 (br s, 1H, NH), 4.7 (m, 1H, CH), 3.80 (s, 3H, OCH₃), 3.3 (m, 2H, CH₂), 3.2 (m, 1H, CH), 2.40 (s, 3H, CH₃). ¹³C NMR (DMSO-d₆) δ : 174.5, 162.8, 160.2, 153.2, 150.5, 140.8, 138.5, 137.2, 131.2, 129.8, 128.5, 126.9. LC-MS m/z 381.13 (M⁺). Anal. Cal. for C₂₀H₂₀N₄O₂S (380.46): C, 63.14; H, 5.30; N, 14.73; O, 8.41; S, 8.43%. Found: C, 63.10; H, 5.34; N, 14.72; O, 8.40; S, 8.46%.

6-((4-chlorobenzylidene)amino)-5-(3-methoxyphenyl)-1,3a,6,7a-tetrahydrothiazolo5,4-d]pyrimidin-7(2H)-one (6l). Yield: 78%. M.P.: 244-246°C. IR (KBr) ν_{\max} (cm⁻¹): 1638 (C=N), 1686 (C=O), 1218-1012 (C-O, methoxy), 772 (C-Cl). ¹H NMR (400 MHz) (CDCl₃) δ (ppm): 8.26 (s, 1H, CH=N-), 7.3-7.9 (m, 8H, Ar-H), 6.8 (m, 1H, Ar-H), 5.6 (br s, 1H, NH), 4.3 (m, 1H, CH), 3.86 (s, 3H, OCH₃), 3.9 (m, 2H, CH₂), 3.5 (m, 1H, CH). ¹³C NMR (DMSO-d₆) δ : 174.1, 162.9, 160.5, 153.0, 150.2, 140.2, 134.8, 133.2, 130.5, 129.8. LC-MS m/z 381.13 (M⁺). Anal. Cal. for C₁₉H₁₇ClN₄O₂S (400.88): C, 56.93; H, 4.27; Cl, 8.84; N, 13.98; O, 7.98; S, 8.00%. Found: C, 56.92; H, 4.26; Cl, 8.80; N, 13.96; O, 7.94; S, 8.02%.

Biology

Tested microorganisms

The antimicrobial activity was evaluated against Gram-positive bacteria *Bacillus subtilis* and *Staphylococcus aureus*, Gram-negative bacteria *Escherichia coli* and *Pseudomonas aeruginosa*, and fungal strains *Candida albicans* and *Fusarium oxysporum*. All microbial strains were obtained from the Department of Microbiology, Shobhit University, Uttar Pradesh, India, and maintained as laboratory reference strains according to standard microbiological procedures prior to biological evaluation.

Preparation of inoculums

Bacterial inoculums were prepared by cultivating the selected strains (*Bacillus subtilis*, *Staphylococcus aureus*, *Escherichia coli*, and *Pseudomonas aeruginosa*) in Mueller Hinton Broth (MHB, HiMedia) at 37°C for 24 hours. The resulting cell suspensions were then diluted with sterile MHB to achieve an approximate concentration of 10⁴ CFU/mL. Fungal strains (*Candida albicans* and *Fusarium oxysporum*) were cultured on Sabouraud Dextrose Agar (SDA) slants at 28°C for 10 days. The spores or yeast cells were harvested using sterile double distilled water and thoroughly homogenized to prepare uniform inoculums.

Agar well diffusion assay

The antimicrobial activity of the twelve synthesized compounds was evaluated using the agar well diffusion method, as previously described by²⁹. Sterile Mueller-Hinton Agar (MHA) plates were prepared by pouring 20 mL of the medium into sterile Petri dishes. After solidification, the surfaces of the agar plates were uniformly inoculated with microbial suspensions using sterile cotton swabs. The plates were allowed to dry for 10 minutes under aseptic conditions.

Wells of 6 mm diameter were punched into the agar using a sterile cork borer, and 100 μ L of each synthesized compound (at a concentration of 1000 μ g/mL) was introduced into the respective wells. Streptomycin (10 μ g/mL) was used as a positive control for antibacterial activity, and Amphotericin B (10 μ g/mL) was used for antifungal activity. Wells filled with the respective solvents were used as negative controls.

The plates were allowed to stand at room temperature for 30 minutes to facilitate diffusion of the test substances into the agar. Subsequently, bacterial plates were incubated at 37°C for 24 hours, and fungal plates at 27°C for 48 hours. After incubation, the antimicrobial activity was assessed by measuring the diameter of the zone of inhibition (in millimeters) around each well. All experiments were conducted in duplicate, and the average results were recorded.

Minimum inhibitory concentration (MIC)

The minimum inhibitory concentration (MIC) of the synthesized compounds **6a-1** was determined using the standard broth microdilution method for antibacterial and antifungal evaluation, as described in literature³⁰. Each compound was initially dissolved in 2% DMSO and serially diluted to obtain final concentrations of 1000, 500, 250, 125, 62.5, 31.25, and 15.62 μ g/mL. The assay was performed in sterile 96-well microtiter plates containing Mueller-Hinton Broth (MHB) for bacterial strains and Sabouraud Dextrose Broth (SDB) for fungal strains. Each well was inoculated with 100 μ L of microbial suspension, adjusted to approximately 1 \times 10⁶ CFU/mL for bacteria and

1×10^4 CFU/mL for fungi. Streptomycin (10 $\mu\text{g/mL}$) and Amphotericin B (10 $\mu\text{g/mL}$) were used as positive controls for antibacterial and antifungal activity, respectively. Wells containing only the respective broth and 2% DMSO were used as negative and solvent controls. After inoculation, the plates were incubated at 37°C for 24 hours for bacterial strains and at 27°C for 48 hours for fungal strains. Following incubation, 5 μL from each well was spot-inoculated onto sterile Mueller-Hinton Agar (for bacteria) or Sabouraud Dextrose Agar (for fungi) and further incubated under respective conditions to confirm growth inhibition. The MIC was recorded as the lowest concentration of the test compound that completely inhibited visible microbial growth. All assays were performed in duplicate to ensure reproducibility.

1,1-Diphenyl-1-picrylhydrazyl (DPPH) radical scavenging assay

The antioxidant potential of the synthesized compounds **6a-l** was evaluated by measuring their hydrogen atom or electron-donating ability using the DPPH (1,1-diphenyl-2-picrylhydrazyl) radical scavenging assay, following a previously reported method with slight modifications³¹. The assay is based on the bleaching of the deep violet color of the DPPH methanolic solution upon reduction by antioxidant compounds. In this method, 1 mL of various concentrations of each test compound (25, 50, 75, 100, and 250 $\mu\text{g/mL}$) prepared in methanol was added to 4 mL of a 0.004% (w/v) methanolic DPPH solution. The reaction mixtures were incubated at room temperature in the dark for 30 minutes. After incubation, the absorbance was recorded at 517 nm using a UV-Visible spectrophotometer against a blank (methanol). Ascorbic acid was used as the standard antioxidant for comparison. A control was prepared by mixing 1 mL of methanol (without any test compound) with 4 mL of DPPH solution. The percentage of DPPH radical scavenging activity (% inhibition) was calculated using the previously reported formula.

Computational drug evaluation

Docking study

Prior to synthesis, molecular docking studies were carried out using the Schrödinger Molecular Modeling Suite to evaluate the binding potential of the designed compounds against antibacterial targets. The crystal structures of DNA gyrase subunit B (PDB ID: 3LD6) and topoisomerase IV subunit C (PDB ID: 3SRW) were downloaded from the Protein Data Bank (<http://www.rcsb.org>). Protein structures were prepared using the Protein Preparation Wizard in Maestro, which involved assigning bond orders, removing water molecules and heteroatoms, adding hydrogen atoms, optimizing hydrogen bond networks, and minimizing the structures using the OPLS3e force field. The active sites were defined based on co-crystallized ligand positions

or literature-reported catalytic residues, following the protocol reported in our previous study³². The 2D structures of the designed compounds were drawn using ChemDraw and converted to 3D structures. These were further processed using the LigPrep module to generate low-energy conformers and appropriate ionization states at physiological pH (7.0 ± 0.5). Docking simulations were performed using the Glide module in Standard Precision (SP) mode. The best binding poses were selected based on GlideScore, and their binding orientations were retained for subsequent analysis. This *in silico* screening approach guided the selection of compounds for synthesis based on their predicted binding affinities and key interactions with the active site residues.

In silico ADME prediction

In silico ADME (Absorption, Distribution, Metabolism, and Excretion) studies were carried out to evaluate the drug-likeness and pharmacokinetic properties of the designed compounds prior to synthesis. The calculations were performed using the QikProp module of the Schrödinger Molecular Modeling Suite.

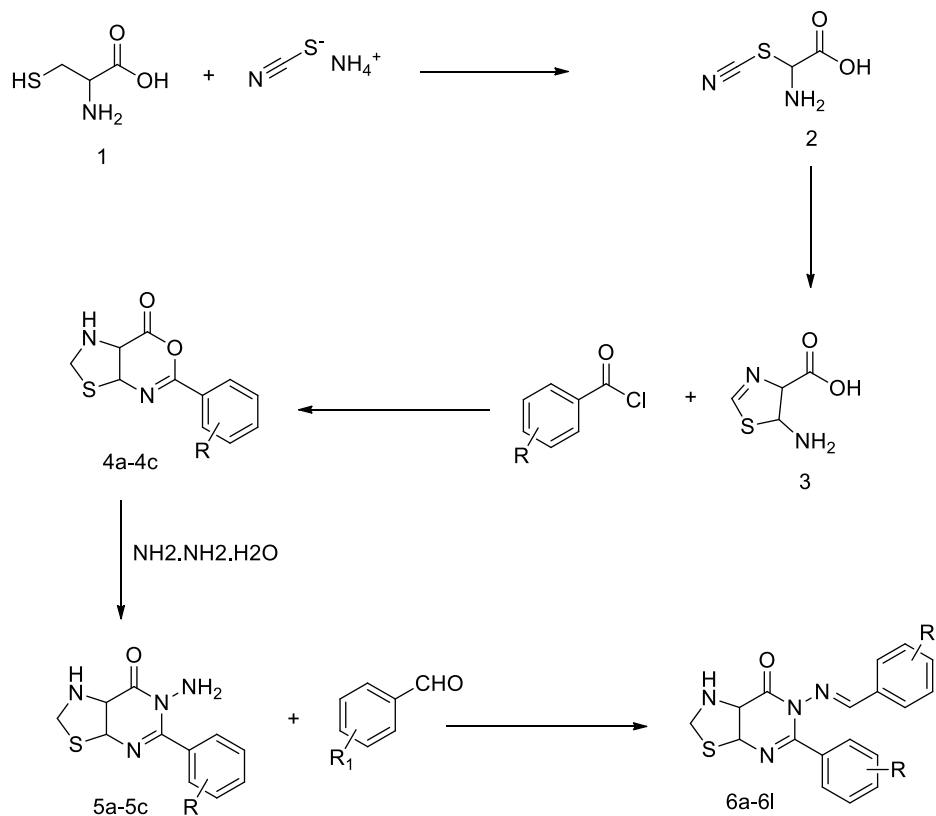
The 2D structures of the compounds were drawn using ChemDraw and converted into 3D structures using LigPrep, ensuring proper stereochemistry and ionization at physiological pH (7.0 ± 0.5). The optimized structures were then submitted to QikProp to predict key ADME-related parameters, including log P (octanol/water partition coefficient), log S (aqueous solubility), log BB (blood-brain barrier permeability), log K_{hsa} (serum protein binding affinity), Caco-2 cell permeability, and percent human oral absorption. Drug-likeness was assessed based on Lipinski's Rule of Five, and all predicted properties were compared against recommended ranges for orally active drugs. These ADME predictions helped to prioritize compounds with favorable pharmacokinetic profiles for synthesis and biological screening.

RESULTS AND DISCUSSION

Chemistry

The synthetic pathway adopted for the preparation of the target thiazolopyrimidinone Schiff bases (**6a-l**) is outlined in **Scheme 1**. The synthesis commenced with the thiocyanation of 2-amino-3-mercaptopropanoic acid, which upon base-mediated nucleophilic substitution with ammonium thiocyanate afforded 2-amino-2-thiocyanatoacetic acid (**2a**) in good yield. Cyclization of **2a** under reflux in aqueous medium produced 5-amino-4,5-dihydrothiazole-4-carboxylic acid (**3a**) through intramolecular attack of the amino group on the thiocyanate carbon, confirming literature-reported thiazole ring formation.

Subsequent acylation of **3a** with substituted benzoyl chlorides followed by intramolecular cyclodehydration



Scheme 1. Synthetic pathway for intermediates (**2a–5c**) and final thiazolopyrimidinone Schiff bases (**6a–l**). Reagents and conditions: (a) NH₄SCN, NaOH, DMSO, 90 °C; (b) H₂O, reflux; (c) substituted benzoyl chloride, TEA, DCM, rt; (d) POCl₃, toluene, reflux; (e) NH₂NH₂·H₂O, EtOH, reflux; (f) substituted benzaldehydes, AcOH, EtOH, reflux.

using POCl₃ furnished a series of phenyl-substituted thiazolo5,4-d[1,3]oxazin-7-ones (**4a–c**). Cyclization was smooth, giving moderate to excellent yields across all derivatives. Treatment of the oxazinone intermediates (**4a–c**) with hydrazine hydrate under reflux resulted in ring opening and rearrangement to afford the corresponding thiazolopyrimidinone derivatives (**5a–c**). The formation of the pyrimidine ring system was confirmed by the appearance of characteristic NH and C=N functional group signals in FTIR and ¹H/¹³C NMR spectra.

Final condensation of **5a–c** with various substituted benzaldehydes in ethanol under acidic conditions successfully yielded the desired thiazolopyrimidinone Schiff bases (**6a–l**). Schiff base formation was evident from the appearance of a strong C=N stretching band in the IR spectra (1640–1655 cm⁻¹) and a singlet in the ¹H NMR spectra corresponding to the azomethine proton (δ 8.1–8.4 ppm). All synthesized compounds exhibited molecular ion peaks consistent with their proposed structures in LC-MS analysis, and elemental analysis values were within acceptable limits.

Overall, the multistep synthetic strategy proved

efficient and reproducible, providing a versatile platform for structural diversification at both the aromatic and heterocyclic moieties. The presence of electron-donating and electron-withdrawing substituents was well tolerated throughout the reaction sequence, enabling the generation of a structurally diverse library for subsequent biological evaluation.

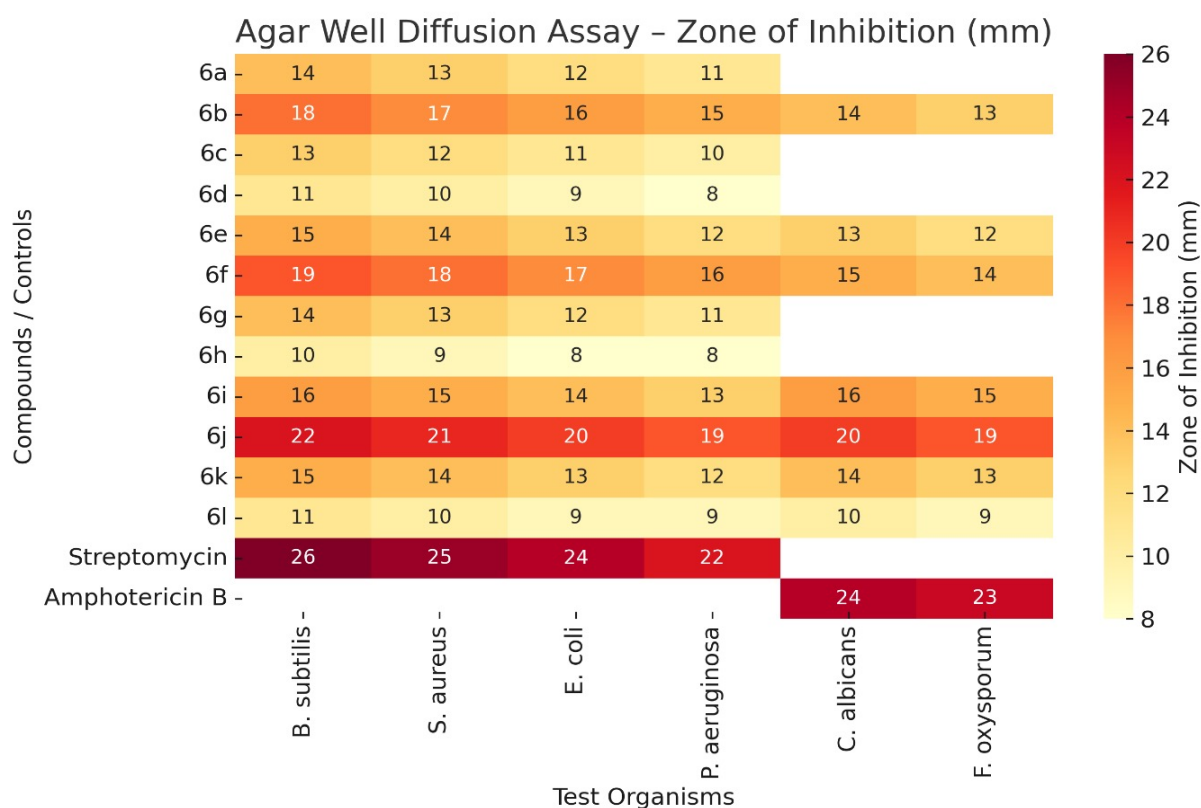
Antimicrobial activity

The antimicrobial activity of the synthesized thiazolopyrimidinone Schiff bases (**6a–l**) was evaluated against a panel of bacterial and fungal strains using the agar well diffusion method. The zone of inhibition results are summarized in **Table 1**, while the overall activity profile is visually represented in the heat map in **Fig. 1**.

As shown in **Table 1** and **Fig. 1**, compounds **6b**, **6f**, and **6j**, containing electron-donating substituents such as -OH or -OCH₃, demonstrated the highest antibacterial activity, particularly against *Staphylococcus aureus* and *Bacillus subtilis*. Their enhanced potency may be attributed to increased electron density on the aromatic ring, facilitating stronger ligand-receptor interactions. Halogen-substituted

Table 1. *In-vitro* antimicrobial activity of thiazolopyrimidinone Schiff bases (6a-l) expressed as zone of inhibition (mm) against gram-positive, gram-negative, and fungal strains

Compound	<i>B. subtilis</i>	<i>S. aureus</i>	<i>E. coli</i>	<i>P. aeruginosa</i>	<i>C. albicans</i>	<i>F. oxysporum</i>
6a	12.5	12	11.5	9	12	10.5
6b	18	18.5	16	13.5	17	14.5
6c	12	12	11.5	9	12	10.5
6d	12.5	12.5	11.5	9	12	10.5
6e	15	15	13.5	11	14	12.5
6f	12.5	12.5	11.5	9.5	12	10.5
6g	15.5	15.5	13.5	11	14.5	12.5
6h	12	12	11.5	9	12	10.5
6i	12	12	11.5	9	12	10.5
6j	19	19	16.5	14	17.5	15
6k	15	15	13.5	11	14	12.5
6l	18	17	16	13.5	16.5	14.5
Streptomycin (10 µg/mL)	26	25	22	20	-	-
Amphotericin B (10 µg/mL)					26	24

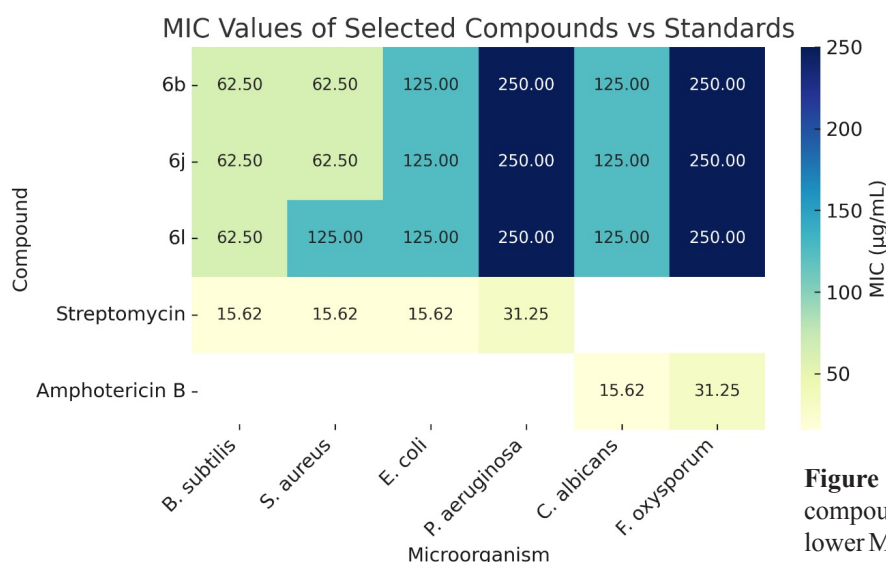
**Figure 1.** Heat map illustrating antimicrobial activity (zone of inhibition) of compounds (6a-l). Higher intensity color corresponds to higher inhibition

derivatives (6d, 6h, 6l) exhibited moderate inhibition, while unsubstituted analogues (6a, 6e, 6i) were comparatively less active. Gram-negative bacteria showed lower susceptibility overall, with *Pseudomonas aeruginosa* being the least responsive across the series.

The minimum inhibitory concentration (MIC) values, presented in **Table 2**, further support these observations. The corresponding MIC heat map (**Fig. 2**) clearly indicates that **6b**, **6f**, and **6j** possess the lowest MIC values (62.5-125 µg/mL) against gram-positive strains, confirming their

Table 2. MIC values ($\mu\text{g/mL}$) of compounds 6a-l determined by broth microdilution assay against bacterial and fungal strains

Compound	<i>B. subtilis</i>	<i>S. aureus</i>	<i>E. coli</i>	<i>P. aeruginosa</i>	<i>C. albicans</i>	<i>F. oxysporum</i>
6b	62.5	62.5	125	250	125	250
6j	62.5	62.5	125	250	125	250
6l	62.5	125	125	250	125	250
6e	125	125	250	500	250	500
6g	125	125	250	500	250	500
6k	125	125	250	500	250	500
6a	250	250	500	500	500	500
6c	250	250	500	500	500	500
6d	250	250	500	500	500	500
6f	250	250	500	500	500	500
6h	250	250	500	500	500	500
6i	250	250	500	500	500	500
Streptomycin (control)	15.62	15.62	15.62	31.25	-	-
Amphotericin B (control)					15.62	31.25

**Figure 2.** Heat map showing MIC values of compounds 6a-l. Darker shades represent lower MIC and therefore higher antimicrobial potency

superior intrinsic antimicrobial potency. Gram-negative strains required higher MIC concentrations, again reflecting their reduced permeability and efflux-based resistance mechanisms.

A similar trend was observed in the antifungal assay (Table 1, Fig. 1). The hydroxy- and methoxy-containing derivatives showed pronounced activity against *Candida albicans* and *Fusarium oxysporum*, whereas halogenated derivatives displayed moderate inhibition. The MIC results in Table 2 and Fig. 2 reinforce this pattern, with 6b, 6f, and 6j exhibiting the lowest MIC values among all synthesized compounds.

Overall, the SAR trend indicates that electron-donating substituents on the benzylidene ring significantly enhance

both antibacterial and antifungal activity, consistent with their favorable docking interactions and predicted pharmacological profiles.

Docking study

Molecular docking studies were performed to understand the binding affinity and interaction modes of the synthesized thiazolopyrimidinone Schiff bases (6a-l) toward two key antimicrobial targets, DNA Gyrase B (PDB ID: 3SRW) and Topoisomerase IV (PDB ID: 3LD6). Docking scores, binding energies, and predicted hydrogen-bond interactions are summarized in Table 3. Overall, compounds 6b, 6j, 6d, and 6l exhibited the most favorable binding energies toward both targets. Among them, compound 6j showed

Table 3. Docking scores, binding energies, and predicted ligand-residue interactions of compounds 6a-l with DNA Gyrase B (3SRW) and Topoisomerase IV

Compound	Docking Scores		Docking Energy		Ligand Efficiency		H-bond count	
	3SRW	3LD6	3SRW	3LD6	3SRW	3LD6	3SRW	3LD6
6a	-6.56	-6.95	-36.45	-32.91	-0.27	-0.29	1	1
6b	-8.07	-7.22	-44.50	-36.87	-0.32	-0.29	1	1
6c	-6.33	-6.94	-36.79	-33.78	-0.25	-0.28	0	1
6d	-6.70	-7.94	-37.19	-38.57	-0.27	-0.32	0	3
6e	-7.62	-6.97	-37.52	-32.19	-0.30	-0.28	0	0
6f	-6.74	-6.49	-38.05	-36.98	-0.26	-0.25	0	2
6g	-7.74	-6.20	-37.33	-30.59	-0.30	-0.24	0	0
6h	-6.41	-7.55	-33.36	-35.89	-0.25	-0.29	0	1
6i	-6.27	-6.30	-36.51	-33.66	-0.24	-0.24	0	1
6j	-8.39	-7.52	-45.69	-40.65	-0.31	-0.28	1	1
6k	-7.28	-6.45	-41.53	-36.11	-0.30	-0.24	1	1
6l	-8.05	-6.57	-40.74	-37.04	-0.27	-0.24	0	2

the strongest affinity for DNA Gyrase B (-8.39 kcal/mol) and Topoisomerase IV (-7.52 kcal/mol), followed closely by **6b** (-8.07 and -7.22 kcal/mol, respectively). These high docking scores indicate that both ligands fit well within the ATP-binding cavity of the enzymes and can potentially inhibit their catalytic function.

The 2D and 3D binding interaction diagrams of compounds **6b** and **6j** with both targets are shown in **Fig. 3** and **Fig. 4**. Compound **6b** forms key hydrogen bonds with amino-acid residues located in the active pocket of 3SRW and 3LD6, along with hydrophobic and π - π stacking interactions that stabilize the ligand orientation. The presence of an electron-donating substituent enhances electron density on the aromatic ring, improving π -interaction complementarity with aromatic residues in the enzyme cavity. Compound **6j**, the best-performing ligand, establishes multiple hydrogen bonds with essential residues in both DNA Gyrase B and Topoisomerase IV. Its methoxy substituent contributes to increased electron donation, improving hydrogen-bond formation and enhancing van der Waals contacts within the hydrophobic core of the binding site. The extended conjugation and flexible framework allow **6j** to adopt an energetically favorable orientation, explaining its superior binding score.

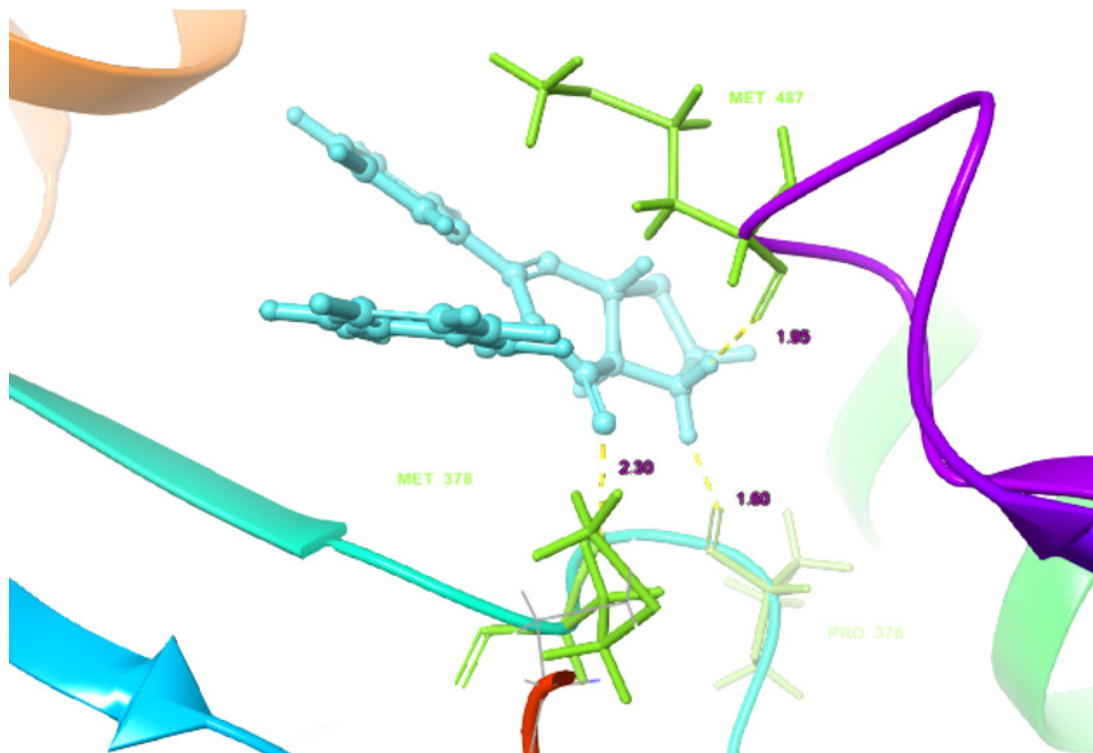
The docking predictions showed excellent agreement with the experimental antimicrobial results. Compounds **6b**, **6f**, and **6j**, which displayed the highest *in vitro* antimicrobial activity (**Table 1**, **Fig. 1**), also exhibited the best docking scores (**Table 3**). In particular, **6j**, which showed the lowest MIC values experimentally (**Table 2**, **Fig. 2**), also demonstrated the strongest binding affinity for both molecular targets. This direct correspondence between computational and biological data confirms that the electron-donating substituents play a pivotal role in enhancing ligand-enzyme interactions. Compounds with

moderate docking scores (such as **6d** and **6l**) also showed moderate antimicrobial activity, while the least active molecules had weaker binding affinities. Thus, the docking study supports the SAR trends of the synthesized analogues and validates **6b** and **6j** as promising lead candidates for further antimicrobial development.

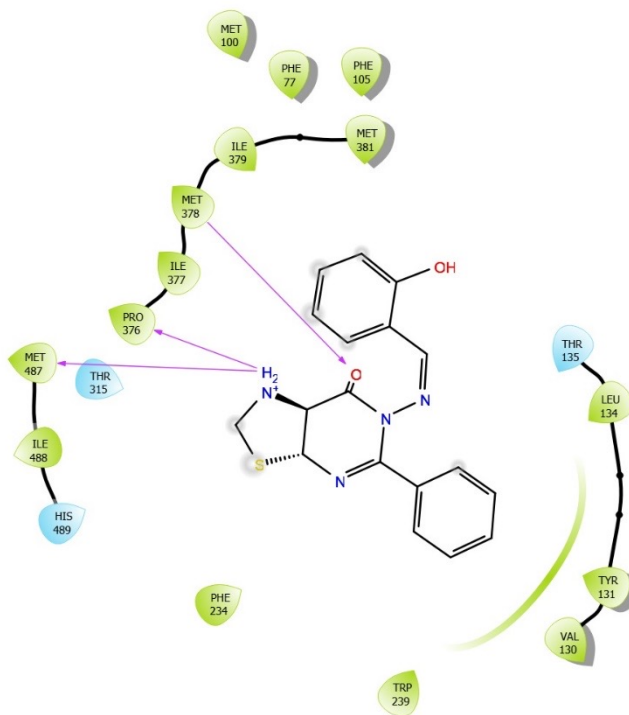
In silico ADME prediction

The *in-silico* ADME properties of compounds **6a-6l** were calculated to evaluate their physicochemical suitability and oral drug-likeness. The results are summarized in **Table 4**. All compounds had molecular weights ranging between **336-400 g/mol**, which is within the acceptable range for good oral bioavailability. Lipophilicity values (logP) were found between **2.62-3.81**, indicating moderate hydrophobicity compatible with passive membrane diffusion. Hydrogen-bond donor (HBD = 1-2) and acceptor counts (HBA = 5.5-7) for all compounds complied with Lipinski's Rule of Five, with *zero violations* reported for the entire series.

The predicted% oral absorption ranged from 85.92% to 100%, demonstrating excellent oral absorption potential across all derivatives. Compounds **6a**, **6c**, **6d**, **6e**, **6g**, **6h**, **6i**, **6k**, and **6l** exhibited >95% oral absorption, whereas compounds **6b**, **6f**, and **6j** showed slightly lower—but still high—absorption values (~86-90%). Rotatable bonds (4-6) suggested acceptable molecular flexibility, supporting good membrane permeability. Permeability assessment using PCaco values revealed high transport potential for most molecules, especially **6a** (568.63 nm/s), **6c** (528.11 nm/s), **6d** (566.42 nm/s), and **6e** (**562.33 nm/s**), all exceeding the threshold for good intestinal permeability. Compounds **6b** (278.56 nm/s) and **6j** (293.38 nm/s) showed moderate PCaco values but still fall within the drug-like range.



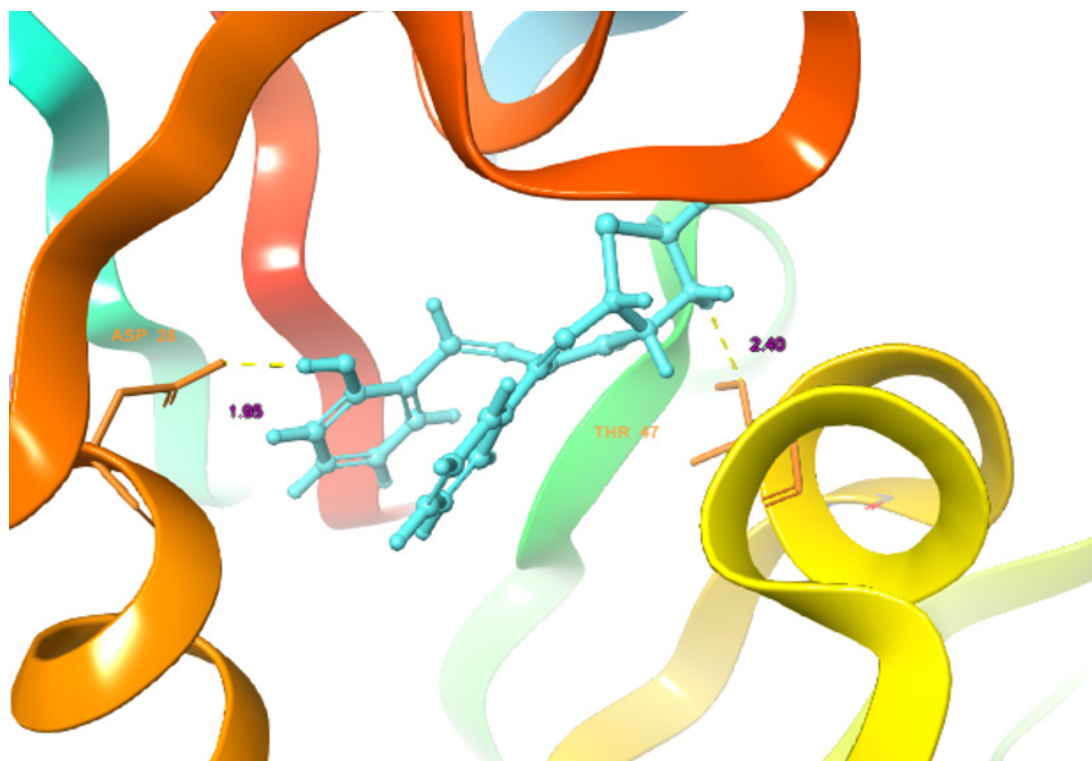
Compound 6b: 3ld6_3D



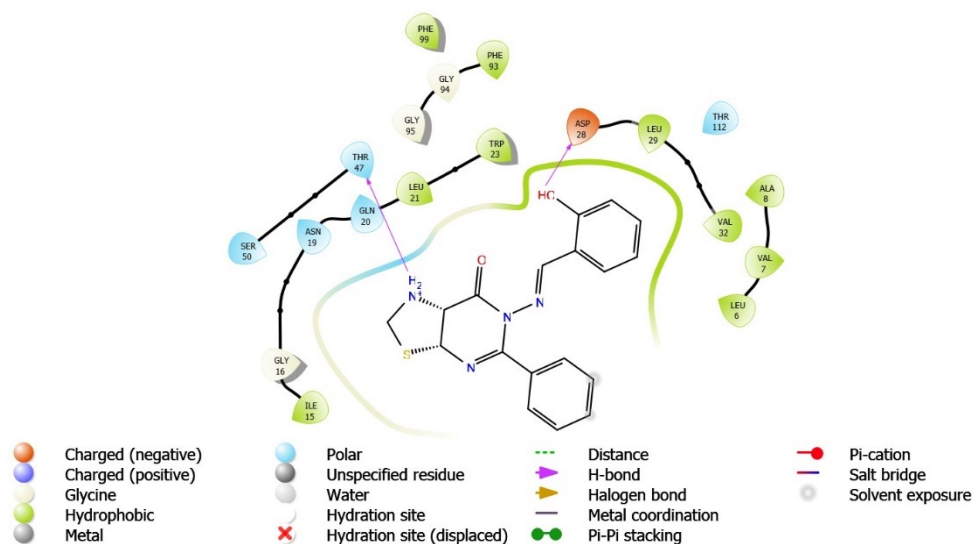
- | | | | |
|--------------------|----------------------------|--------------------|------------------|
| Charged (negative) | Polar | Distance | Pi-cation |
| Charged (positive) | Unspecified residue | H-bond | Salt bridge |
| Glycine | Water | Halogen bond | Solvent exposure |
| Hydrophobic | Hydration site | Metal coordination | |
| Metal | Hydration site (displaced) | Pi-Pi stacking | |

Compound 6b: 3ld6_2D

Figure 3. *cont.*



Compound 6b: 3srw_3D



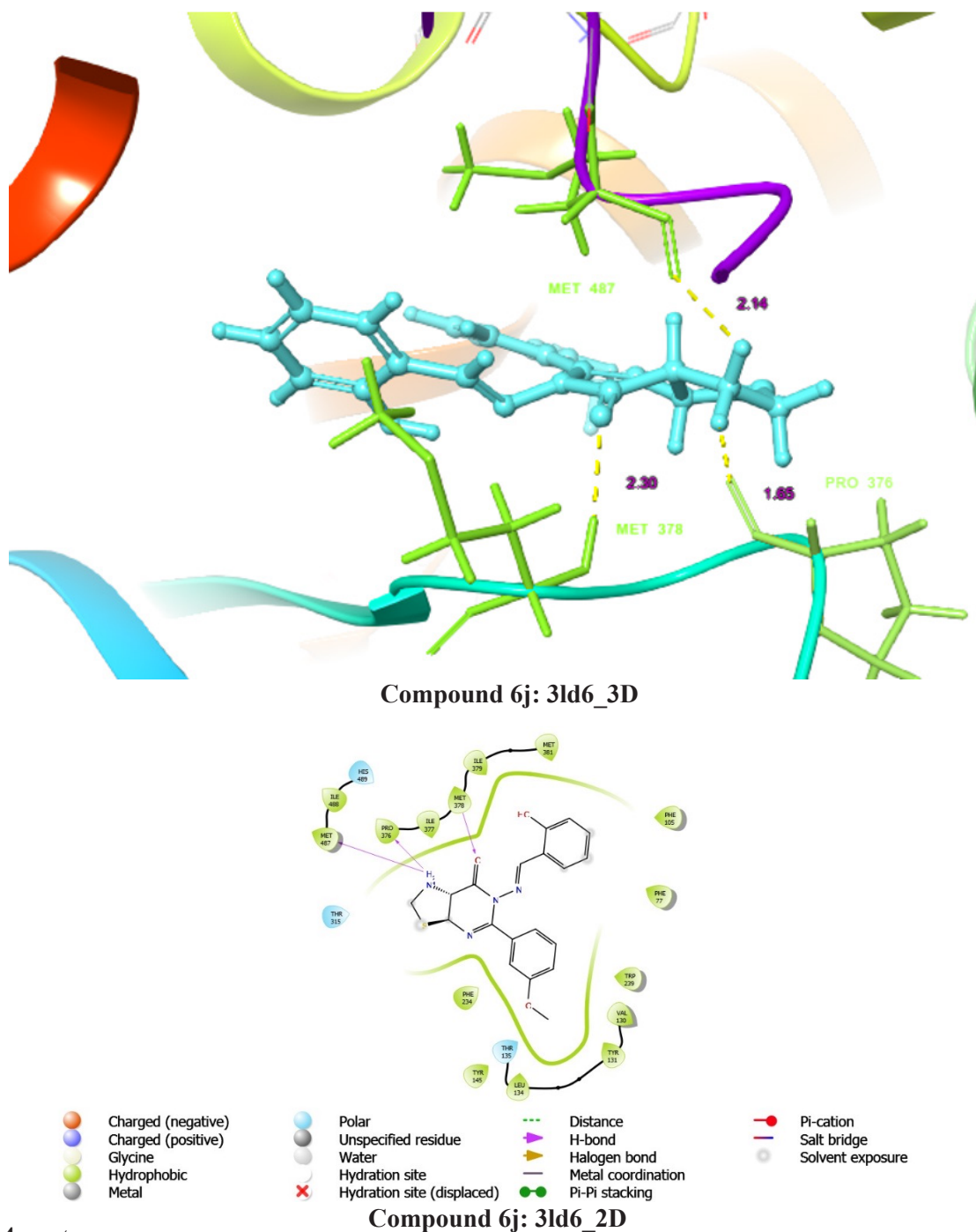
Compound 6b: 3srw_2D

Figure 3. 2D and 3D binding interactions of compound **6b** with Topoisomerase IV (3LD6) and DNA Gyrase B (3SRW)

Predicted logBB values (-0.24 to 0.38) suggest that some derivatives such as **6d** and **6h** may have moderate CNS penetration, whereas others remain largely peripheral. Cardiac toxicity risk predicted by logHERG values (-5.84 to -6.68) indicates that all compounds are within the acceptable non-blocker range, suggesting a low likelihood of hERG channel inhibition. Importantly, none of the compounds showed any Lipinski violations, implying good

oral drug-likeness and favorable physicochemical traits for further development.

Among the evaluated molecules, compounds **6b**, **6f**, and **6j** demonstrated an optimal balance of lipophilicity ($\log P < 3$), acceptable PCaco permeability, good oral absorption, and no toxicity alerts—correlating with their superior antimicrobial and antioxidant activities. These findings indicate that the structural features contributing to strong

Figure 4. *cont.*

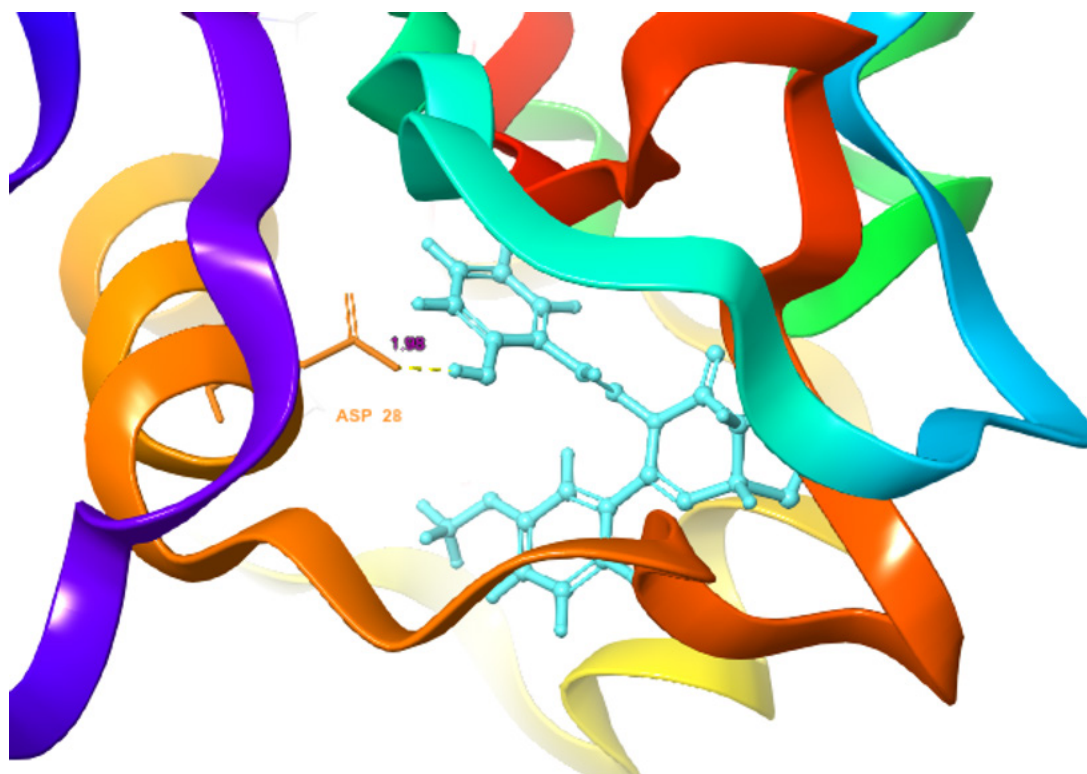
biological activity also support favorable ADME behavior.

CONCLUSIONS

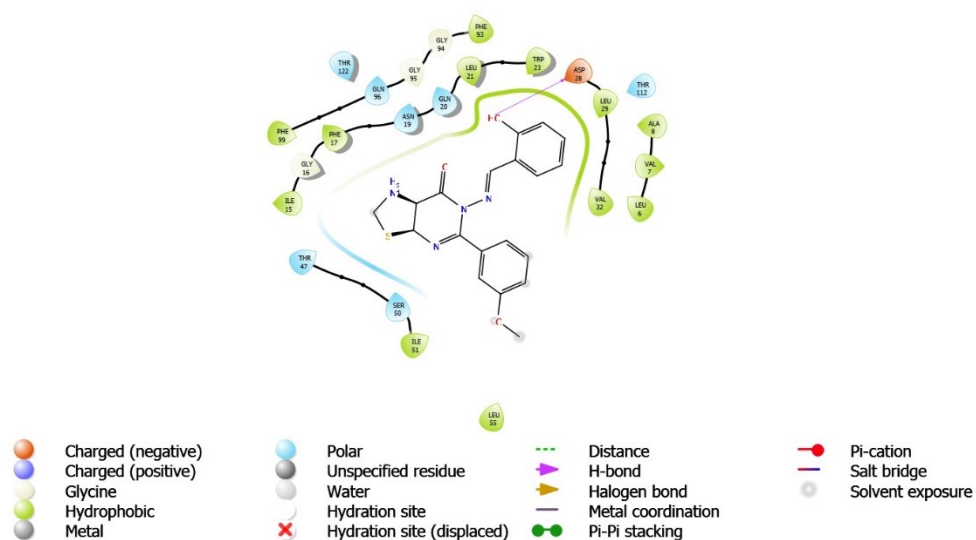
In this study, a new series of thiazolopyrimidinone Schiff bases (6a-6l) was successfully designed, synthesized, and evaluated for their antimicrobial, antioxidant, molecular docking, and *in-silico* ADME properties. Several compounds demonstrated promising biological activity, among which **6b**, **6f**, and **6j** emerged as the most potent

antimicrobial and antioxidant agents. These derivatives showed significant inhibitory effects against both bacterial and fungal strains, with low MIC values and strong dose-dependent DPPH scavenging activity.

Molecular docking studies further supported the experimental findings, revealing that compounds **6b** and **6j** exhibited the highest binding affinities toward DNA Gyrase B (3SRW) and Topoisomerase IV (3LD6). Their favourable binding conformations, characterized by multiple hydrogen



Compound 6j: 3srw_3D



Compound 6j: 3srw_2D

Figure 4. 2D and 3D binding interactions of compound **6j** with Topoisomerase IV (3LD6) and DNA Gyrase B (3SRW)

bonds and hydrophobic interactions, correlate well with their superior *in vitro* activity. In-silico ADME evaluation indicated that all synthesized molecules possess acceptable physicochemical properties, high predicted oral absorption, and compliance with Lipinski's rule, suggesting good drug-likeness. Notably, compounds **6b**, **6f**, and **6j** exhibited a balanced ADME profile consistent with their biological performance.

Overall, the integration of synthetic chemistry, biological screening, computational modelling, and ADME prediction highlights **6b**, **6f**, and **6j** as promising lead candidates for further optimization. These findings provide a valuable foundation for the development of new antimicrobial and antioxidant agents based on the thiazolopyrimidinone scaffold.

Table 4. Predicted in-silico ADME properties of compounds 6a-6l including molecular weight, dipole moment, rotatable bonds, hydrogen bond donors/acceptors, logP, logHERG, PCaco permeability, logBB, % oral absorption, and Lipinski Rule of Five compliance. Values obtained from ADMET modeling analysis

Compound	Mol. Wt.	Dipole	Rot. bonds	HB donor	HB acceptor	log Po/w	log HERG	PCaco	log BB	% Oral Absorption	Rule of Five
6a	336.41	6.07	4	1	5.5	3.07	-6.17	568.63	0.23	94.21	0
6b	352.41	5.32	5	2	6.25	2.62	-6.45	278.56	-0.17	85.92	0
6c	350.44	5.43	4	1	5.5	3.49	-6.56	528.11	0.14	96.80	0
6d	370.86	3.79	4	1	5.5	3.73	-6.55	566.42	0.35	98.85	0
6e	350.44	5.60	4	1	5.5	3.42	-6.34	562.33	0.20	97.61	0
6f	366.44	4.33	5	2	6.25	2.85	-5.84	439.15	0.05	90.65	0
6g	364.46	4.54	4	1	5.5	3.53	-5.91	553.27	0.19	98.13	0
6h	384.88	4.31	4	1	5.5	3.81	-5.98	562.47	0.38	100.00	0
6i	366.44	6.33	5	1	6.25	3.36	-6.68	509.86	0.06	95.00	0
6j	382.44	5.00	6	2	7	2.76	-6.44	293.38	-0.24	87.23	0
6k	380.46	6.01	5	1	6.25	3.55	-6.55	548.27	0.08	98.01	0
6l	400.88	4.33	5	1	6.25	3.68	-6.46	539.74	0.25	98.85	0

CONFLICT OF INTEREST STATEMENT

The authors declare that there is no conflict of interest regarding the publication of this article.

ACKNOWLEDGEMENT

The School of Pharmaceutical Education and Research at Jamia Hamdard, New Delhi Facilitated this work by offering the essential resources for the docking studies.

REFERENCES

1. **Yaoa, X., Hub, H., Wang, S., Zhao, W., Songb, M. and Zhou, Q. (2021).** Synthesis, Antimicrobial Activity, and Molecular Docking Studies of Aminoguanidine Derivatives Containing an Acylhydrazone Moiety. *IJPR*. 20: 536-545.
2. **Zezelew, D., Endale, M., Melaku, Y., Demissie, T.B. and Eswaramoorthy, R.L.K. (2022).** ZnO Nanoparticle-Assisted Synthesis of Thiazolo[3,2- α] Pyrimidine Analogs: Antibacterial and Antioxidant Activity, In Silico Molecular Docking, and ADMET Prediction Study. *Journal of Chemistry*. 1346856.
3. **Morjana, R.Y., El-Hallaqb, A.F., Azaraha, J.N., Almasric, I.M., Alzaharnad, M.M., Al-Reefie, M.R., Beadhamf, I., Abu-Teimb, Q.S., Elmanamad, A.A., Awadallaha, A.M., Raffertye, J., Gardinerg, J.M. (2023).** Synthesis, docking and evaluation of novel fused pyrimidine compounds as possible lead compounds with antibacterial and antitumor activities. *Journal of Molecular Structure*. 1288: 135754.
4. **Shaabana, O.G., Issac, D.A.E., El-Tombarya, A.A., El Wahabd, S.M.A., Wahabe, A.E.A., Abdelwahab, I.A. (2019).** Synthesis and molecular docking study of some 3,4-dihydrothieno[2,3-d] pyrimidine derivatives as potential antimicrobial agents. *Bioinorganic Chemistry*. 88: 102934.
5. **Bai, X.Q., Shi Li, C., Cui, M.Y., Song, Z., Yu Zhou, X., Zhang, C., Zhao, Y., Zhang, T., Jiang, T.Y. (2019).** Synthesis and molecular docking studies of novel pyrimidine derivatives as potential antibacterial agents. *Molecular Diversity*.
6. **Jampilek, J. (2019).** Heterocycles in Medicinal Chemistry. *Molecules*. 24: 3839.
7. **Ammara, Y.A., Farag, A.A., Ali, A.M., Ragaba, A., Ahmed A.A. Elsisib, D.M., Belald, A. (2020).** Design, synthesis, antimicrobial activity and molecular docking studies of some novel di-substituted sulfonol quinoxaline derivatives. *Bioinorganic Chemistry*. 104: 104164.
8. **Kamal, A., Khan, M.N.A., Reddy, K.S., Rohini, K., Sastry, G.N., Sateesh, B. and Sridhar, B. (2007).** Synthesis, structure analysis, and antibacterial activity of some novel 10-substituted 2-(4-piperidyl/phenyl)-5,5 dioxo 1,2,4] triazolo[1,5-b][1,2,4] benzothiadiazine derivatives. *Bioorg. Med. Chem. Lett*. 17: 5400-5405.
9. **Frank, E. and Szollosi, G. (2021).** Nitrogen-Containing Heterocycles as Significant Molecular Scaffolds for Medicinal and Other Applications. *Molecules*. 26: 4617.
10. **Üstün, E., Sahin N., Özdemir, I., Günal, S., Gürbüz, N., Özdemir, I., Sémeril, D. (2023).** Design, synthesis, antimicrobial activity and molecular docking study of cationic is-benzimidazole-silver(I) complexes. *Arch Pharm*. 2300302.
11. **Fahim, M.A., Farag, A.M., (2020).** Synthesis, antimicrobial evaluation, molecular docking and theoretical calculations of novel pyrazolo[1,5-a] pyrimidine derivatives. *Journal of Molecular Structure*. 1199 (2020) 127025.
12. **Prabhala, P., Savanur, H.K.M., Sutar, S.M., Naik, K.N., Mittal, M.K., Kalkhambkar, R.G. (2024).** In silico molecular docking and In vitro antimicrobial evaluation of some C5-substituted imidazole analogues. *European Journal of Medicinal Chemistry Reports*. 3: 100015.
13. **Horchani, M., Hajlaoui, A., Harrath, A.H., Mansour, L., Jannet, H.B., Romdhane, A. (2020).** New pyrazolo-triazolo-pyrimidine derivatives as antibacterial agents: Design and synthesis, molecular docking and DFT studies.

- Journal of Molecular Structure. 1199: 127007.
14. **Digafie, Z., Melaku, Y., Belay, Z. and Eswaramoorthy, R. (2021).** Synthesis, Molecular Docking Analysis, and Evaluation of Antibacterial and Antioxidant Properties of Stilbenes and Pinacol of Quinolines. *Hindawi*. 6635270.
 15. **Hossan, A., Alshahag, M., Alisaac, A., Bamaga, M.A., Alalawy, A.I. and El-Metwaly, N.M. (2023).** Synthesis, molecular modelling and biological evaluation of new 4-aminothiophene and thiopyrimidine compounds. *Journal of Taibah University for Science*. 17: 2164993.
 16. **Radwan, M.A.A., Alshubramy, M.A., Motaal, M.A., Hemdan, B.A., El-Kady, D.S. (2019).** Synthesis, molecular docking and antimicrobial activity of new fused Pyrimidine and Pyridine derivatives. *Bioorganic Chemistry*. 96: 103516.
 17. **Othman, I.M.M. Alamshany, Z.M., Tashkandi, N.Y., Gad-Elkareema, M.A.M., Anwar, M.M., Nossier, E.S. (2021).** New pyrimidine and pyrazole-based compounds as potential EGFR inhibitors: Synthesis, anticancer, antimicrobial evaluation and computational studies. *Bioorganic Chemistry*. 114: 105078.
 18. **Ghoneim, A.A., Zafar, R. and Farargy, A.F.F. (2021).** Design, Synthesis, Molecular Docking and Antimicrobial Activity of Novel Thiazolo 5,4 c] Pyridine Glycoside and Thiazolo4,5-d] Pyrimidin Glycoside. *Polycyclic Aromatic Compounds*. 1903953.
 19. **Desai, N.C., Harsora, J.P., Monapara, J.D. and Khedkar, V.M. (2021).** Synthesis, Antimicrobial Capability and Molecular Docking of Heterocyclic Scaffolds Clubbed by 2 Azetidinone, Thiazole and Quinoline Derivatives. *Polycyclic Aromatic Compounds*. 1877747.
 20. **Naglah, A.M., Askar, A.A., Al-Omar, M.A., Hassan, A.S. and Bhat, M.A. (2020).** Biological Evaluation and Molecular Docking with In Silico Physicochemical, Pharmacokinetic and Toxicity Prediction of Pyrazolo[1,5-a] pyrimidines. *Molecules*. 25: 1431.
 21. **Hassan, A.S., Askar, A.A., Nossier, E.S., Naglah, A.M., Moustafa, G.O. and Al-Omar, M.A. (2019).** Antibacterial Evaluation, In Silico Characters and Molecular Docking of Schi Bases Derived from 5-aminopyrazoles. *Molecules*. 24: 3130.
 22. **Sutradhar, R.K., Marma, A., Hossain, M.E. (2024).** Synthesis, Bioactivity Screening and Docking Analysis of Thiazole Derivatives Containing Quinoline Moieties. *Oriental Journal of Chemistry*. 40: 1297-1305.
 23. **Pibiri, I. (2024).** Recent Advances: Heterocycles in Drugs and Drug Discovery. *Int. J. Mol. Sci.* 25: 9503.
 24. **Morjana, R.Y., El-Hallaq, A.F., Azaraha, J.N., Almasric, I.M., Alzaharnad, M.M., Al-Reefie, M.R., Beadhamf, I., Abu-Teimb, O.S., Elmanamad, A.A., Awadallaha, A.M., Rafterye, J., Gardinerg, J.M. (2023).** Synthesis, docking and evaluation of novel fused pyrimidine compounds as possible lead compounds with antibacterial and antitumor activities. *Journal of Molecular Structure*. 1288: 135754.
 25. **Shaabana, O.G., Issac, D.A.E., El-Tombarya, A.A., El Wahabd, S.M.A., Wahabe, A.E.A., Abdelwahab, L.A. (2019).** Synthesis and molecular docking study of some 3,4-dihydrothieno[2,3-d] pyrimidine derivatives as potential antimicrobial agents. *Bioinorganic Chemistry*. 88: 102934.
 26. **Hossan, A., Alshahag, M., Alisaac, A., Bamaga, M.A., Alalawy, A.I. and El-Metwaly, N.M. (2023).** Synthesis, molecular modelling and biological evaluation of new 4-aminothiophene and thiopyrimidine compounds. *Journal of Taibah University for Science*. 17: 2164993.
 27. **Othmana, I.M.M., Alamshanyb, Z.M., Tashkandib, N.Y., Gad-Elkareema, M.A.M., Anwar, M.M., Nossier, E.S. (2021).** New pyrimidine and pyrazole-based compounds as potential EGFR inhibitors: Synthesis, anticancer, antimicrobial evaluation and computational studies. *Bioorganic Chemistry*. 114: 105078.
 28. **Prabhala, P., Savanur, H.K.M., Sutar, S.M., Naik, K.N., Mittal, M.K., Kalkhambkar, R.G. (2021).** In silico molecular docking and *In vitro* antimicrobial evaluation of some C5-substituted imidazole analogues. *European Journal of Medicinal Chemistry Reports*. 3: 100015.
 29. **Valgas, C., Souza, S.M., Smânia, E.F.A., Smânia, A. (2007).** Screening Methods To Determine Antibacterial Activity Of Natural Products. *Brazilian Journal of Microbiology*. 38: 369-380.
 30. **Ping, X., Zhang, M., Sheng, R., Ma, Y. (2017).** Synthesis and biological evaluation of deferiprone-resveratrol hybrids as antioxidants, A β 1-42 aggregation inhibitors and Metal-chelating agents for Alzheimer's disease. *European Journal of Medicinal Chemistry*. 127: 174-186.
 31. **Williams, W.B., Cuvelier, M.E. and Berset, C. (1995).** Use of a Free Radical Method to Evaluate Antioxidant Activity. *Lebanism. -Wiss. U.-Technol.* 30: 28.25.
 32. **Azmat, K.M. Chauhan, B., Naseer, M.A., Kumar, N., Ali, Z. (2025).** Design, Synthesis, Molecular Docking and Antimicrobial Activity of New Thiazole-Fused Pyrimidine Derivatives. *Asian Journal of Chemistry*. 37: 680-688.